RSC Advances

ROYAL SOCIETY OF CHEMISTRY

www.rsc.org/advances

ARTICLE TYPE www. rsc.org/xxxxxx | XXXXXXXX

Intrinsic carrier mobility of germanene is larger than graphene's: first-principle calculations

Xue-Sheng Ye,[a] Zhi-Gang Shao,*[a] Hongbo Zhao,[a] Lei Yang,[a,b] and Cang-Long Wang[a]

Received Xth XXXXXXXXXX 20XX, Accepted Xth XXXXXXXXX 20XX
First published on the web Xth XXXXXXXXXX 20XX
DOI: 10.1039/b000000x

Shown here is the intrinsic carrier mobility (ICM) of germanene, a group-IV graphene-like two-dimensional buckled nanosheet. Specifically, combining the Boltzmann transport equation with relaxation time approximation at the first-principle level, it was calculated that the ICM of the germanene sheet can reach $\sim 6\times10^5 cm^2V^{-1}s^{-1}$, in an order of magnitude$(10^5 cm^2V^{-1}s^{-1})$, and even larger than that of graphene. The high ICM of germanene is attributed to the large buckled distance and the small effective mass. Since Ge has good compatibility with Si in the conventional semi-conductor industry, the results manifest that germanene should be a good supplement in prospective nanoelectronics.

1 Introduction

Graphene, the two-dimensional (2D) honeycomb network of carbon atoms, has become the most investigated material due to its fascinating properties, such as its linearly dispersing electronic bands at Fermi level contributing to its high carrier mobility.[1–3] The group IV elements graphene-like 2D sheets, such as those formed from Si and Ge, named silicene and germanene, respectively, have attractive fundamental physical and chemical properties[4–10], and can easily fit into the silicon-based electronic industry. Thereinto, silicene has been synthesized by the epitaxial growth of Si on Ag(110), and Ag(111).[4,11–17] Recently, germanene has also attracted intense studies, where germanene with a low-buckled structure has been predicted to be stable[5,18–24] and semimetallic[7]. Lately, Bianco *et al.* have synthesized and characterized the germanane (hydrogenated germanene).[3,21] What is more, since the exciton Bohr radius (23.4 nm) in bulk Ge crystal is much longer than that (4.9 nm) in bulk Si crystal[25,26], Ge nanomaterials will be more affected by those sizes than Si nanomaterials.[25] Due to its good compatibility with Si and high carrier mobility, Ge has potential advantages for improving performance of silicon-based electronic devices.[4,6–8,27–29]

As a matter of fact, intrinsic carrier mobility (ICM) of materials is the crucial factor for semiconducting materials.[6,30–32] Previously, the first-principle methodology, developed by the group of Shuai, incorporating the density functional theory, the Boltzmann transport equation, and the deformation potential (DP) theory has been carried out to predict ICM of many organic materials.[31–36] We have predicted that the ICM of silicene reaches $2.5\times10 cm^2V^{-1}s^{-1}$ with the same first-principle methodology.[37] In addition, theoretical calculations show that germanene also has graphene-like electronic band structure, resulting in charge carriers behaving as massless Dirac fermions. Moreover, the buckled structure leads to reduction of electron-phonon coupling strength. Therefore, the buckled structure should affect the ICM of germanene strongly.

Hence, we predict the ICM of germanene using the first-principle methodology incorporating band structure calculations with the density functional theory and the Boltzmann transport equation under the DP theory.[31–36] We have also investigated the influence of buckled structure on the ICM of germanene. Our results can shed new light on ICM of materials and be used as a guide for further experimental nanoelectronics.

2 Model and methods

Figure 1 shows the low-buckled structure of germanene. In order to present more intuitive explanation for transport property, we build a super-cell along two vertical directions **a** and **b** in the charge transport calculation.[33] **a** and **b** are the directions of dilation. Dark dashed lines label the rectangle supercell, where the lattice constants are $a_0 = 4.03$Å and $b_0 = 6.97$Å at equilibrium geometry. Geometry optimization and the band structure calculations are performed using density-functional theory as implemented in CASTEP package[38]. Perdew-Burke-Ernzerhof (PBE) functional[39] within the generalized gradient approximation (GGA) is taken into account to deal with exchange and correlation term. For

[a] *Laboratory of Quantum Engineering and Quantum Materials, SPTE, South China Normal University and Institute of Modern Physics, Chinese Academy of Sciences, Guangzhou 510006, China. Corresponding E-mail:zgshao@scnu.edu.cn*
[b] *Department of Physics, Lanzhou University, Lanzhou 730000, China*

germanene, a plane wave basis set with the energy cutoff of 500eV and Vanderbilt ultrasoft pseudopotential[40] are applied. The Brillouin zone is sampled by a $49 \times 49 \times 1$ Monkhorst-Pack mesh of k-point[41]. The vacuum layer thickness is 16 Å. The calculated bond length and low-buckled distance of germanene are 2.42 Å and 0.69 Å, respectively, which are in good agreement with the calculated values in Ref. 5. The low-buckled distance of germanene is higher than that of silicene ($0.37 \sim 0.46$ Å).[5,42,43]

According to the aforementioned first-principle method[31–37], the relaxation time of carriers of germanene can be expressed as

$$\frac{1}{\tau_\alpha(i,\mathbf{k})} = K_B T \frac{2\pi E_1^2}{\hbar C_\alpha} \sum_{k' \in BZ} \left\{ \left[1 - \frac{V_\alpha(i,\mathbf{k}')}{V_\alpha(i,\mathbf{k})} \right] \delta\left[\varepsilon(i,\mathbf{k}') - \varepsilon(i,\mathbf{k})\right] \right\} \quad (1)$$

where α represents the direction of dilation. $\tau_\alpha(i,\mathbf{k})$, $V_\alpha(i,\mathbf{k})$ and $\varepsilon(i,\mathbf{k})$ are the relaxation time, the group velocity, and band energy at the k-point of the ith band, respectively. E_1 is the DP constant, C_α is the 2D elastic constant.

Incorporating the Boltzmann transport theory with relaxation time approximation, the ICM μ can be derived as

$$\mu_\alpha^{e(h)} = \frac{e}{K_B T} \frac{\sum_{i \in CB(VB)} \int \tau_\alpha(i,\mathbf{k}) V_\alpha^2(i,\mathbf{k}) f_0^{e(h)}(\varepsilon) d\mathbf{k}}{\Sigma_{i \in CB(VB)} \int f_0^{e(h)}(\varepsilon) d\mathbf{k}} \quad (2)$$

where $f_0 = (1 + exp[(\varepsilon - \varepsilon_F)/K_B T])^{-1}$ is the Fermi-Dirac distribution function. h and e indicate hole and electron, respectively. $V(i,\mathbf{k})$ is the group velocity defined as $V(i,\mathbf{k}) = \nabla_k \varepsilon(i,\mathbf{k})/\hbar$.

3 Results and discussion

The band structure and density of states (DOS) of the germanene sheet are shown in Fig. 2. The k-point separation of 10^{-3}Å^{-1} on the Brillouin zone path is taken to calculate accurately the group velocity.[37,41,44,45] It can be seen from the Fig. 2 that the germanene has Dirac cones, which is consistent with previous studies[5,19,46,47]. The linearly dispersing electronic bands at the Fermi level causes the carriers to behave as Dirac fermions[17] at the speed about $3.8 \times 10^5 ms^{-1}$.[48] For the transport calculation, we dilate the super-cell of germanene along the axis **a** or **b** in the range of $\pm 1.5\%$.[31–35] In order to obtain the relaxation time of germanene, we have calculated the Fermi level shift ΔE and the total energy (E) of the super-cell as functions of the dilation. The relationship between the Fermi level shift ΔE and the dilation is plotted in Fig. 3(a), which is fitted linearly as $\Delta E = E_1(\Delta l/l_0)$. And the relationship between total energy and the dilation is plotted in Fig. 3(b), which is fitted parabolically as $(E - E_0)/S_0 = C_\alpha(\Delta l/l_0)^2/2$. C_α is the elastic constant and $\Delta l/l_0$ describes the dilation. E_0,

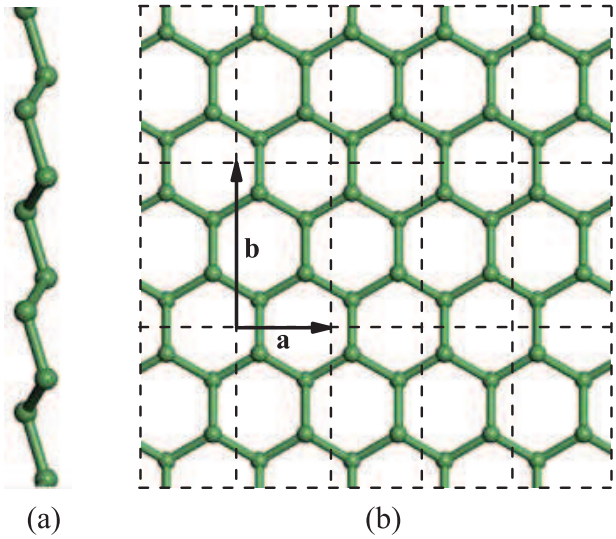

Fig. 1 Side (a) and top (b) views of schematic diagram of the germanene sheet. **a** and **b** are the directions of dilation. The rectangle supercell (drawn with dark dashed line) are labeled.

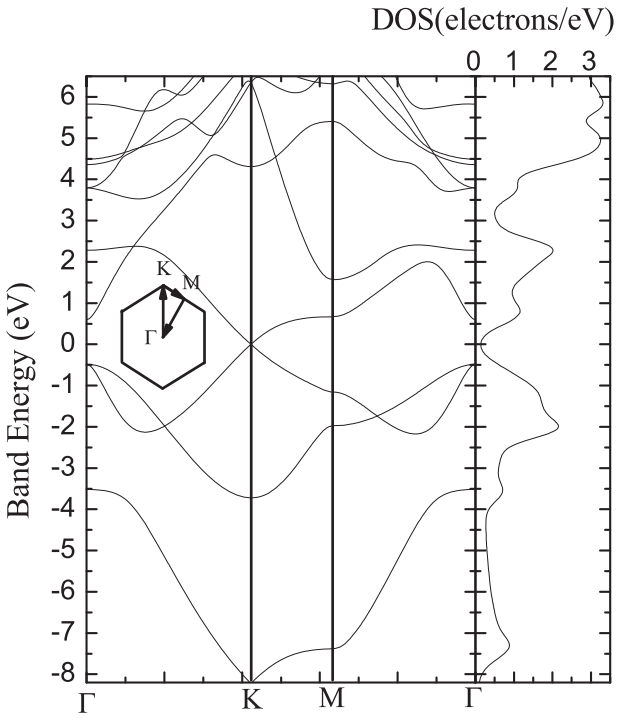

Fig. 2 Band structure and DOS of the germanene sheet.

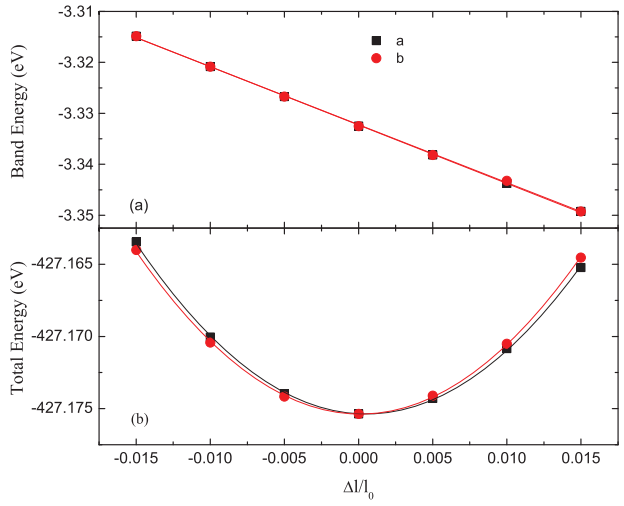

Fig. 3 Fermi level shift (a) and the total energy (b) as functions of the lattice dilation $\Delta l/l_0$ along the directions of *a* and *b* for germanene. The linear fit gives the DP constant and the parabola fit gives the elastic constant, respectively.

S_0, and l_0 are the total energy, cell area, and lattice constant, respectively.[31–37]

We obtain the the DP constant E_1 by linearly fitting the data in Fig. 3(a) and the elastic constant C_α by the parabola fitting the data in Fig. 3(b).[31–37] With Eqs. 1 and 2, we calculate the relaxation time and ICM of germanene. The relevant results are summarized in Table 1. We also provide the relevant results of graphene and silicene calculated in previous studies[31–37] for comparison.

The buckled distances of graphene, silicene, and germanene increase successively.[5,42] It is can be seen from Table 1 that the elastic constant decreases as the buckled distance increases. The elastic constant of graphene with no buckled structure is the largest compared with the smallest value of germanene with the highest buckled structure. This result is consistent with the mechanical properties of germanene investigated using Quantum-ESPRESSO package recently, where Si-Si bonds of silicene and Ge-Ge bonds of germanene are more flexible than C-C ones of graphene with the buckled structure[42]. In order to explain how the low buckled distance affects the elastic constant, we calculated bond population of the three honeycomb structures by CASTEP code. It is shown in Table 1 that the larger buckled distance leads to smaller bond population. As the bond population increases, the bond strength increases[49]. As a consequence, the larger bucked distance leads to the smaller elastic constant. Moreover, it also can be found from Table 1 the DP constant decreases as the buckled distances increases. Due to the buckled structure, when the lattice deformation is applied to the silicene and germanene, the bonds are not directly dilated, which can only cause a small band energy shift. In contrast, when the deformation is applied to graphene with no buckled structure, the dilation is directly influence on the bond length, so the corresponding band energy shift is large. A similar explanation has been successfully applied to analyze the difference between the graphynes and graphene.[35]

According to Eq. 1, the relaxation time is proportional to the elastic constant and inversely proportional to the square of the DP constant. Substituting the data in Table l, the values of $\frac{C_\alpha}{E_1^2}$ are 12.42, 19.06, and 41.74 for graphene, silicene, and germanene, respectively. As a consequence, the relaxation time around the Dirac cone of germanene is larger than those of silicene and graphene. The relaxation time of graphene is larger than that of silicene, which is just because the shape of the Dirac cone of graphene is more symmetric than that of silicene. It can be seen from Eq. 2 the ICM depends not only on the relaxation time but also on group velocities and shapes of the Fermi surfaces. However, the group-IV elements graphene-like 2D sheets all have Dirac cones in their Brillouin zones and they all have high Fermi velocities around the Dirac cone about $6.3\times10^5 ms^{-1}$, $5.1\times10^5 ms^{-1}$, and $3.8\times10^5 ms^{-1}$ for graphene, silicene, and germanene, respectively.[48] Therefore, the large relaxation time around the Dirac cone should lead to the high ICM of germanene, shown as in Table 1. In addition, Bardeen and Shockley have pointed out that higher mobilities of electrons and holes in Ge as compared with Si are correlated with a smaller shift of energy gap with dilation[50], which verifies the high ICM of germanene in our results from another perspective.

Moreover, the ICM can be expressed as $\mu = -\frac{e\tau}{m^*}$. As the mean scattering time τ increases or the effective mass m^* decreases, the ICM increases.[34] In Ref. 6, Ni *et al.* have shown the effective mass of germanene is $m_e^{K\Gamma} = 0.014m_0$ and $m_e^{MK} = 0.029m_0$ at $E_\perp = 0.4V/\text{Å}$ is close to the value of bilayer graphene and smaller then the experimental value $m_e = 0.06m_0$ of graphene by Novoselov *et al.*[31]. Hence it is reasonable that the calculated ICM of germanene is larger than that of graphene.

4 Conclusions

In summary, we have predicted the intrinsic carrier mobility (ICM) of germanene based on band structure calculations with the density functional theory, and Boltzmann transport equation coupled with the deformation potential theory at the first-principle level. The ICM of germanene can reach $6.24\times10^5 cm^2V^{-1}s^{-1}$ and $6.54\times10^5 cm^2V^{-1}s^{-1}$ for electrons and holes, respectively, at room temperature. Our results show that calculated ICM of germanene is in the same order of magnitude of that in graphene and silicene, which originates from

Table 1 Bond Population *BP*, Buckled Distance Δh(Å), Lattice Constants L(Å), DP Constant $E_1(eV)$, Elastic Constant $C_\alpha(Jm^{-2})$, Relaxation Time near Dirac cone $\tau_D(ps)$ and ICM $\mu(10^5 cm^2V^{-1}s^{-1})$ of electrons and holes along the **a** and **b** directions at 300K for germanene, silicene, and graphene sheets.

system	BP	Δh	axis	L	E_1	C_α	τ_D^e	τ_D^h	μ^e	μ^h
germanene	2.04	0.69	a	4.03	1.16	56.01	5.26	5.46	6.09	6.39
			b	6.97	1.15	55.98	5.39	5.58	6.24	6.54
silicene[37]	2.73	0.44	a	3.88	2.13	86.48	1.84	1.84	2.58	2.23
			b	6.71	2.13	85.99	1.83	1.83	2.57	2.22
graphene[34]	3.05	0	a	2.46	5.14	328.02	2.24	2.27	3.39	3.22
			b	4.26	5.00	328.30	2.37	2.40	3.20	3.51

the effect of the buckled distance and the small effective mass. From the Table 1, it is clear to find the ICM of germanene even larger than that of graphene and silicene. Within the DP theory, we only take the scattering of a thermal electron or hole by acoustic phonon into account.[34] Under the circumstances, it is even more remarkable that the ICM of germanene is in an order of magnitude ($10^5 cm^2V^{-1}s^{-1}$). Recently, some studies by first-principle calculations have demonstrated that graphene and h-BN are suitable substrates to synthesize germanene[23,24]. For example, Cai et al. show germanene can be stable and preserve its linear energy and low-buckled structure on the substrate of graphene[24]. And, Li et al. show that germanene can stably attach on h-BN substrate via Van der Waals interactions and the high carrier mobility of germanene can be well preserved in that situation.[23] The most important thing is that the substrate can open the bandgap in germanene.[6,23,24] So germanene is suitable for semiconductor industry. Nevertheless, for real application in nanoelectronics the ICM of germanene with the induced substrate needs further research. In any event, since it has the high ICM and good compatibility with Si, germanene will be a good supplement in nanoelectronics.

Acknowledgement

Zhi-Gang Shao acknowledges the support by the National Natural Science Foundation of China (Grant Nos. 11105054 and 11274124) and PCSIRT (Grant No. IRT1243) and by the high-performance computing platform of South China Normal University. Hongbo Zhao acknowledges the support by the National Natural Science Foundation of China (Grant No. 91026005). Lei Yang acknowledged also the support by the National Natural Science Foundation of China (Grant No. 11074077) and the "Strategic Priority Research Program" of the Chinese Academy of Sciences (Grant No. XDA03030100). Cang-Long Wang acknowledges the support by the National Natural Science Foundation of China (Grant No. 11304324).

References

1 K. S. Novoselov, A. K. Geim, S. V. Morozov, D. Jiang, Y. Zhang, S. V. Dubonos, I. V. Grigorieva and A. A. Frisov, *Science*, 2004, **306**, 666–669.
2 K. S. Novoselov, A. K. Geim, S. V. Morozov, D. Jiang, M. I. Katsnelson, I. V. Grigorieva, S. V. Dubonos and A. A. Frisov, *Nature*, 2005, **438**, 197–200.
3 E. Bianco, S. Butler, S. Jiang, O. D. Restrepo, W. Windl and J. E. Goldberger, *ACS Nano*, 2013, **7**, 4414–4421.
4 P. De Padova, C. Quaresima, C. Ottaviani, P. M. Sheverdyaeva, P. Moras, C. Carbone, D. Topwal, B. Olivieri, A. Kara, H. Oughaddou, B. Aufray and G. Le Lay, *Appl. Phys. Lett.*, 2010, **96**, 261905.
5 S. Cahangirov, M. Topsakal, E. Aktürk, H. Şahin and S. Ciraci, *Phys. Rev. Lett.*, 2009, **102**, 236804.
6 Z. Ni, Q. Liu, K. Tang, J. Zheng, J. Zhou, R. Qin, Z. Gao, D. Yu and J. Lu, *Nano Lett.*, 2012, **12**, 113–118.
7 M. Houssa, G. Pourtois, V. Afanasev and A. Stesmans, *Appl. Phys. Lett.*, 2010, **96**, 082111.
8 X.-Q. Wang, H.-D. Li and J.-T. Wang, *Phys. Chem. Chem. Phys.*, 2012, **14**, 3031–3036.
9 L. Stille, C. J. Tabert and E. J. Nicol, *Phys. Rev. B*, 2012, **86**, 195405.
10 L. Matthes, O. Pulci and F. Bechstedt, *J. Phys.: Condens. Matter*, 2013, **25**, 395305.
11 B. Aufray, A. Kara, S. Vizzini, H. Oughaddou, C. Leandri, B. Ealet and G. Le Lay, *Appl. Phys. Lett.*, 2010, **96**, 183102.
12 B. Lalmi, H. Oughaddou, H. Enriquez, A. Kara, S. Vizzini, B. Ealet and B. Aufray, *Appl. Phys. Lett.*, 2010, **97**, 223109.
13 A. Kara, H. Enriquez, A. P. Seitsonen, L. Lew Yan Voon, S. Vizzini, B. Aufray and H. Oughaddou, *Surf. Sci. Rep.*, 2012, **67**, 1–18.
14 P. De Padova, O. Kubo, B. Olivieri, C. Quaresima, T. Nakayama, M. Aono and G. Le Lay, *Nano Lett.*, 2012, **12**, 5500–5503.
15 B. Feng, Z. Ding, S. Meng, Y. Yao, X. He, P. Cheng, L. Chen and K. Wu, *Nano Lett.*, 2012, **12**, 3507–3511.
16 P. Vogt, P. De Padova, C. Quaresima, J. Avila, E. Frantzeskakis, M. C. Asensio, A. Resta, B. Ealet and G. Le Lay, *Phys. Rev. Lett.*, 2012, **108**, 155501.
17 L. Chen, C.-C. Liu, B. Feng, X. He, P. Cheng, Z. Ding, S. Meng, Y. Yao and K. Wu, *Phys. Rev. Lett.*, 2012, **109**, 056804.
18 G. G. Guzmán-Verri and L. C. Lew Yan Voon, *Phys. Rev. B*, 2007, **76**, 075131.
19 C.-C. Liu, W. Feng and Y. Yao, *Phys. Rev. Lett.*, 2011, **107**, 076802.
20 F. Bechstedt, L. Matthes, P. Gori and O. Pulci, *Appl. Phys. Lett.*, 2012, **100**, 261906.
21 K. J. Koski and Y. Cui, *ACS Nano*, 2013, **7**, 3739–3743.
22 D. Kaltsas and L. Tsetseris, *Phys. Chem. Chem. Phys.*, 2013, **15**, 9710–9715.
23 L. Li and M. Zhao, *Phys. Chem. Chem. Phys.*, 2013, **15**, 16853–16863.
24 Y. Cai, C.-P. Chuu, C. M. Wei and M. Y. Chou, *Phys. Rev. B*, 2013, **88**, 245408.

25 H. Zhou, M. Zhao, X. Zhang, W. Dong, X. Wang, H. Bu and A. Wang, *J. Phys.: Condens. Matter*, 2013, **25**, 395501.
26 Y. Wu and P. Yang, *Chem. Mater.*, 2000, **12**, 605–607.
27 Q. Pang, Y. Zhang, J.-M. Zhang, V. Ji and K.-W. Xu, *Nanoscale*, 2011, **3**, 4330–4338.
28 W. Wei, Y. Dai, B. Huang and T. Jacob, *Phys. Chem. Chem. Phys.*, 2013, **15**, 8789–8794.
29 X.-Q. Wang, H.-D. Li and J.-T. Wang, *Phys. Chem. Chem. Phys.*, 2012, **14**, 3031–3036.
30 J. Wang, R. Zhao, M. Yang, Z. Liu and Z. Liu, *J. Chem. Phys.*, 2013, **138**, 084701.
31 M.-Q. Long, L. Tang, D. Wang, L. Wang and Z. Shuai, *J. Amer. Chem. Soc.*, 2009, **131**, 17728–17729.
32 Z. Shuai, L. Wang and Q. Li, *Adv. Mater.*, 2011, **23**, 1145–1153.
33 M. Long, L. Tang, D. Wang, Y. Li and Z. Shuai, *ACS Nano*, 2011, **5**, 2593–2600.
34 J. Xi, M. Long, L. Tang, D. Wang and Z. Shuai, *Nanoscale*, 2012, **4**, 4348–4369.
35 J. Chen, J. Xi, D. Wang and Z. Shuai, *J. Phys. Chem. Lett.*, 2013, **4**, 1443–1448.
36 J. Chen, D. Wang and Z. Shuai, *J. Chem. Theory Comput.*, 2012, **8**, 3338–3347.
37 Z.-G. Shao, X.-S. Ye, L. Yang and C.-L. Wang, *J. Appl. Phys.*, 2013, **114**, 093712.
38 M. D. Segall, P. J. D. Lindan, M. J. Probert, C. J. Pickard, P. J. Hasnip, S. J. Clark and M. C. Payne, *J. Phys.: Condens. Matter*, 2002, **14**, 2717.
39 J. P. Perdew, K. Burke and M. Ernzerhof, *Phys. Rev. Lett.*, 1996, **77**, 3865–3868.
40 D. Vanderbilt, *Phys. Rev. B*, 1990, **41**, 7892–7895.
41 J. D. Pack and H. J. Monkhorst, *Phys. Rev. B*, 1977, **16**, 1748–1749.
42 T. Kaloni and U. Schwingenschlögl, *Chem. Phys. Lett.*, 2013, **583**, 137–140.
43 F.-b. Zheng and C.-w. Zhang, *Nanoscale Res. Lett.*, 2012, **7**, 1–5.
44 G. Kresse and J. Furthmüller, *Phys. Rev. B*, 1996, **54**, 11169–11186.
45 G. Kresse and J. Furthmüller, *Comput. Mater. Sci.*, 1996, **6**, 15–50.
46 K. Takeda and K. Shiraishi, *Phys. Rev. B*, 1994, **50**, 14916–14922.
47 H. Behera and G. Mukhopadhyay, *AIP Conf. Proc.*, 2011, **1349**, 823–824.
48 L. C. Lew Yan Voon, E. Sandberg, R. S. Aga and A. A. Farajian, *Appl. Phys. Lett.*, 2010, **97**, 163114.
49 M. D. Segall, R. Shah, C. J. Pickard and M. C. Payne, *Phys. Rev. B*, 1996, **54**, 16317–16320.
50 J. Bardeen and W. Shockley, *Phys. Rev*, 1950, **80**, 72–80.